

ADVANCES IN QUANTITATIVE EPMA COMPOSITIONAL MAPPING APPLIED TO APOLLO 17 CORE 73002,6015-6018. P.K. Carpenter¹, R.C. Ogliore², A. Minocha², C. J-K. Yen¹, B.L. Jolliff¹, and the ANGSA Science Team³, ¹Dept. of Earth and Planetary Sciences, ²Dept. of Physics and ^{1,2}McDonnell Center for the Space Sciences, Washington University, St. Louis, MO, USA, ³www.lpi.usra.edu/ANGSA/teams/ (paulc@wustl.edu).

Introduction: We present significant advances in fully quantitative compositional mapping and a novel web-based tool *Quantitative Microanalysis Explorer* (QME) for inspecting Apollo 17 core samples 73002,6015-6018, summarized here and described in a companion abstract [1].

Electron Microprobe Imaging and Quantitative Compositional Mapping: The 73002,6015-6018 samples are 50 × 25 mm epoxy grain mounts of regolith, and were analyzed using the JEOL JXA-8200 electron microprobe (EPMA) at Washington University. Approximately 325 backscattered-electron (BSE) images were collected using the JEOL guide-net mapping software, at 15 kV, 2 nA probe current, and 70× magnification, and stitched using the ImageJ Fiji grid-collection stitching plug-in [2], to produce a 20k by 5k BSE mosaic base image with ~ 1.5 μm pixel resolution. For each 73002 slide, five EPMA stage maps were acquired using fixed wavelength-dispersive spectrometers (WDS). Each stage map was acquired at 1024 × 1024 resolution using a step size of 9.5 μm with a fixed 10 μm electron beam at 15 kV, 100 nA probe current, and a dwell time of 25 msec. Two passes were used to collect X-ray intensities for Mg, Al, Fe, Ca, and Ti in pass 1, and Na, Si, Mn, K, and Cr in pass 2. These mapping runs each required 18 hrs. per map, and generated a total of 20 × 10⁶ fully quantitative analyses on all four slides.

The X-ray intensity maps were processed using Probe Software CalcImage and Probe for EPMA, by performing a full $\Phi(\rho z)$ correction at each pixel in the maps [3]. This correction is of the form $C = k \times ZAF$, where C is the element concentration, the k -ratio $k = (P-B)^{std}/(P-B)^{smp}$ is the background corrected relative peak X-ray intensity ($P-B$) at each pixel in the map compared to the calibration standard, and ZAF is the compositionally dependent matrix correction for atomic number Z , X-ray absorption A , and characteristic fluorescence F in both the sample and standard. This full correction is more accurate than methods using uncorrected X-ray intensity measurements or algorithms of the form $C = m \times I + B$, where a linear relationship is presumed between concentration C and X-ray intensity I , and a fixed global background is assumed for all phases in the map. These assumptions are not justified and should not be used for map quantification.

The $\Phi(\rho z)$ correction uses a mean atomic number (MAN) background calibration routinely used for quantitative analysis in our facility. The MAN correction utilizes EPMA standards having a range of average atomic

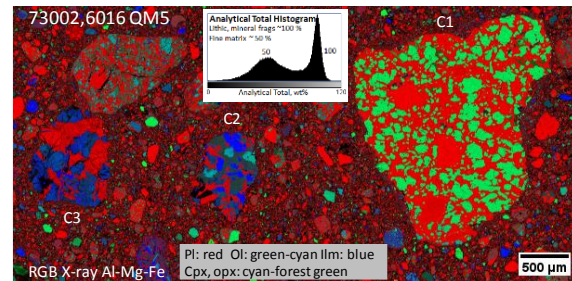


Figure 1. Al-Mg-Fe RGB X-ray map showing clasts 1, 2, and 3 from 73002,6016 quant map 5. Plagioclase is red, olivine and pyroxene are green-blue depending on Mg:Fe. Inset shows analytical total histogram for this map area.

number Z and provides an accurate and internally-consistent background correction. The MAN correction also allows all map collection time to be dedicated to on-peak X-ray measurement which improves precision and detection limits, which are 0.1 – 0.2 element wt.% for all elements in this map set.

The quantitative compositional map data were processed using a set of Matlab routines which generate 32-bit floating point .tiff quantitative map images for element and oxide wt.%, cation stoichiometry, derived mineral end member maps, and input image stacks for ENVI processing [4]. The X-ray intensity maps and quantitative compositional maps were stitched using Fiji and Matlab routines. The resulting single-element and RGB composite X-ray maps are used for comparison with BSE and optical image mosaics for reflected light, plane polarized, and crossed polars. We typically use an Al-Mg-Fe RGB composite X-ray map to discriminate feldspathic (red) and ferromagnesian (green and blue) phases in the core slides (Fig. 1), and compare with the BSE and optical images to discriminate crystalline vs. glassy phases.

Development of web tool: The 73002 sections present a challenge to evaluate wide-area maps and to compare imaging and microanalysis data. We have developed the *Quantitative Microanalysis Explorer* web tool as a cutting-edge interface to the 73002 data set. This web tool performs zoomable map navigation and sequential comparison of BSE, X-ray, optical, and quantitative compositional data for a given field of view. The tool allows extraction of element, oxide, and cation formula data for discrete point, rectangular region, and irregular polygon regions as outlined by the mouse. Extracted quantitative analysis data is copied to the clipboard and can be pasted into Excel for further evaluation.

Discussion: The compositional mapping data we present for 73002 is of high analytical quality and the map data can be used for analysis of a range of materials at different scales [5]. The lunar regolith includes large lithic and mineral fragments as well as fine submicron particles. The analytical total histogram for 73002,6016 QM5 is shown as an inset in Fig. 1, and illustrates excellent totals of ~100 wt.% for well-polished fragments with sufficient surface area to obtain good analyses. The very fine-grained matrix represents single and multiphase materials embedded in casting epoxy, and exhibits analytical totals range around 50 wt. %.

In Fig. 1, clast C1 is a troctolitic granulite breccia consisting of unzoned olivine, plagioclase with variable Na content, and minor Cpx, Opx, and armalcolite. Table 1A compares analyses of several olivine crystals in the clast, using conventional EPMA spot analysis vs. inscribed rectangular regions extracted using the QME tool. This comparison highlights the nature of spot analysis (high analytical quality and few in number, here $n=20$ spots) with mapping results (historically low analytical quality but high in number, here $n=391$ pixels). The excellent agreement demonstrates the high accuracy of analyses in the quantitative mapping data set with data similar to EPMA spot analyses despite two orders of magnitude shorter count times. The accuracy of map analysis improves with the number of pixels selected using the QME tool which has a nominal 25 msec per pixel count time, so that 100 pixels selected is equivalent to 2.5 sec and 1000 pixels is equivalent to 25 sec of total count time. We observe that small numbers of pixels can be used to identify phases and observe local zoning chemistry or quickly compare phases from different clasts.

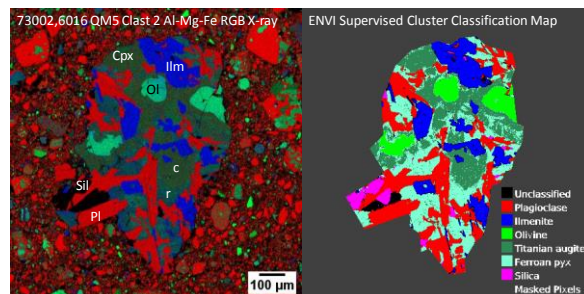


Figure 2. Al-Mg-Fe RGB X-ray map of high-Ti basalt. Ca-pyroxene zoning: cores have elevated Ti, Al, Cr, and Ca compared to rims which have elevated Mg, Fe, and Si. Right image is ENVI classification map used for bulk analysis calculation. Maps acquired at 2.5 μm per pixel and 25 msec for comparison to QME map data set.

Clast C2 is a 0.5 \times 1.0 mm high-Ti basalt lithic fragment. As seen in Fig. 2, this clast contains olivine, zoned Ca-pyroxene with Ti-Al rich cores and ferroan rims, ilmenite, plagioclase, and silica. Modal proportions of these phases were determined by supervised cluster

analysis using ENVI. The cluster map clearly identifies each phase and delineates complex core-rim and crystal growth zoning in Ca pyroxene. The modal abundances have been used to calculate a density-corrected bulk composition. This calculation compares mineral analysis using selected EPMA spots, inscribed rectangular regions using the QME tool, and all pixels using the ENVI cluster analysis. The results are shown in Table 1B, and illustrate several points. First, the QME and ENVI data are of comparable accuracy to EPMA spot analyses, again demonstrating the high analytical quality of each. Second, there is an increase in sampling coverage from the EPMA, QME, and ENVI data with full coverage of all pixels represented by the ENVI calculation. Finally, these results show a very similar composition compared to the 1974 Rose bulk analysis of ilmenite basalt 70017 [6], which demonstrates the capability to quantitatively compare microchemistry with bulk chemistry. In comparison, the sampled cross-section of clast C2 likely has lower modal ilmenite, higher plagioclase, and less ferroan olivine and Ca-pyroxene compared to 70017.

Summary: We discuss significant advances in quantitative EPMA compositional mapping, demonstrate the capabilities of the QME web tool for extraction of data, and apply these methods to the 73002,6015-6018 sections. This set of research tools provides a framework for rapid inspection of materials in the 73002 core and points to a new approach to compositional mapping.

Table 1A			Table 1B			
	EPMA N=20	QME N=391	EPMA	QME	ENVI	70017 Rose 1974
SiO ₂	39.85	39.02	39.16	38.97	38.18	38.80
TiO ₂	0.09	0.10	11.90	11.28	12.14	12.84
Al ₂ O ₃	0.02	0.25	9.06	9.11	9.11	8.54
Cr ₂ O ₃	0.14	0.15	0.36	0.72	0.44	0.49
FeO	14.19	15.62	17.96	17.24	18.17	18.12
MnO	0.16	0.19	0.27	0.25	0.37	0.24
MgO	45.95	45.76	9.56	9.54	9.57	10.16
CaO	0.09	0.21	11.40	12.03	11.45	10.56
Na ₂ O	0.00	0.07	0.37	0.38	0.48	0.33
K ₂ O	0.00	0.03	0.01	0.06	0.09	0.07
Total	100.47	99.50	100.04	99.59	100.00	100.15

Acknowledgements: We thank NASA for loan of the 73002 drive tube continuous core thin sections and for funding via the ANGSA Program (80NSSC19K0958).

References: [1] Minocha A. et al. (2022) *A17-ANGSA Workshop*; [2] Donovan J. et al. (2021) *Am. Mineral.* 106 (11) 171-1735; [3] <https://fiji.sc/>; [4] <https://www.l3harrisgeospatial.com>; [5] Jolliff B.L. et al. (2022) *A17-ANGSA Workshop* [6] <https://curator.jsc.nasa.gov/lunar/lsc/70017.pdf>.